

University of Groningen

Investigating possible bypass mechanisms to sensitize AML blasts for combination therapy

Kampen, Kim Rosalie

IMPORTANT NOTE: You are advised to consult the publisher's version (publisher's PDF) if you wish to cite from it. Please check the document version below.

Document Version

Publisher's PDF, also known as Version of record

Publication date:

2015

[Link to publication in University of Groningen/UMCG research database](#)

Citation for published version (APA):

Kampen, K. R. (2015). *Investigating possible bypass mechanisms to sensitize AML blasts for combination therapy: Targeting ligand induced receptor tyrosine kinase signaling*. [Thesis fully internal (DIV), University of Groningen]. University of Groningen.

Copyright

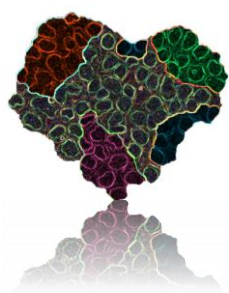
Other than for strictly personal use, it is not permitted to download or to forward/distribute the text or part of it without the consent of the author(s) and/or copyright holder(s), unless the work is under an open content license (like Creative Commons).

The publication may also be distributed here under the terms of Article 25fa of the Dutch Copyright Act, indicated by the "Taverne" license. More information can be found on the University of Groningen website: <https://www.rug.nl/library/open-access/self-archiving-pure/taverne-amendment>.

Take-down policy

If you believe that this document breaches copyright please contact us providing details, and we will remove access to the work immediately and investigate your claim.

Downloaded from the University of Groningen/UMCG research database (Pure): <http://www.rug.nl/research/portal>. For technical reasons the number of authors shown on this cover page is limited to 10 maximum.



6

EphB1 Suppression in Acute Myelogenous Leukemia: Regulating the DNA Damage Control System

K.R. Kampen¹, F.J.G. Scherpen¹, G. Garcia-Manero², H. Yang², G.J.L. Kaspers³, J. Cloos³, C.M. Zwaan⁴, M.M. van den Heuvel-Eibrink⁴, S.M. Kornblau², E.S.J.M. De Bont¹

1. Department of Pediatric Oncology/Hematology, Beatrix Children's Hospital, University Medical Center Groningen, University of Groningen, Groningen, The Netherlands. 2. Department of Leukemia, The University of Texas MD Anderson Cancer Center, Houston, Texas, United States of America. 3. Department of Pediatric Oncology/Hematology, VU University Medical Center, Amsterdam, The Netherlands. 4. Department of Pediatric Oncology/Hematology, Erasmus MC-Sophia Children's Hospital, Rotterdam, The Netherlands.

Mol Cancer Res. 2015 Jun;13(6):982-92

Abstract

Loss of ephrin receptor (EphB1) expression may associate with aggressive cancer phenotypes; however, the mechanism of action remains unclear. To gain detailed insight into EphB1 function in acute myelogenous leukemia (AML), comprehensive analysis of EphB1 transcriptional regulation was conducted. In AML cells, EphB1 transcript was inversely correlated with EphB1 promoter methylation. The presence of EphB1 allowed EphB1 ligand-mediated p53 DNA binding, leading to restoration of the DNA damage response (DDR) cascade by the activation of ATR, Chk1, p53, p21, p38, CDK1(tyr15), and Bax, and downregulation of HSP27 and Bcl2. Comparatively, reintroduction of EphB1 expression in EphB1-methylated AML cells enhanced the same cascade of ATR, Chk1, p21, and CDK1(tyr15), which consequently enforced programmed cell death. Interestingly, in pediatric AML samples, EphB1 peptide phosphorylation and mRNA expression were actively suppressed as compared with normal bone marrow, and a significant percentage of the primary AML specimens had EphB1 promoter hypermethylation. Finally, EphB1 repression associated with a poor overall survival in pediatric AML. Combined, the contribution of EphB1 to the DDR system reveals a tumor-suppressor function for EphB1 in pediatric AML.

Introduction

Ephrin tyrosine kinase receptors take part in the largest family of receptor tyrosine kinases, consisting of cell surface membrane bound kinases that include at least 14 receptors and 8 ligands. The most extensively investigated functions of ephrin receptors and ligands involve cell adhesion and migration via bidirectional signaling. Eph receptors are known for their contradictory function to promote or suppress cancer progression depending on their cellular contexts. EphA1/2/4/5/7 and EphB2/4 receptor overexpression has been shown to contribute to the pathogenesis of tumors with respect to tumor growth, tumor grade, and patient outcome in hepatocellular carcinoma, pancreatic adenocarcinoma, astrocytoma, and gliomas.¹⁻⁵ In contrast, Eph receptors can also fulfill tumor suppressor functions. EphA2 receptor activation has been implicated to function as a tumor suppressor in breast cancer, non-small cell lung carcinoma and prostate cancer cells.⁶⁻⁹ Ephrin-A1 induced activation of EphA2 in breast cancer cells was shown to decrease in vivo tumorigenicity in mouse models.^{10;11} Loss of EphB1 has previously been shown to associate with an aggressive cancer phenotype in gastric carcinoma and serous ovarian cancers.^{12;13} Various mechanisms are described to suppress EphR expression in cancer pathogenesis; transcriptional repression of *EphB2* by *c-REL*, frequent deletion of the chromosomal region 1p36 encounters *EphA2*, *EphA8* and *EphB2* loss in many cancers, or hypermethylation of the CpG Island on the promoter regions resulting in loss of function of *EphB6* in breast cancer, *EphB2* in colorectal cancer and *EphA7* in prostate cancer.^{10;11;14-18} In EfnB1 Lck-Cre KO mice it has been shown that Efn ligands are redundant in expression and functionality in relation to normal lymphoid hematopoiesis.¹⁹ In contrast, in acute lymphoid leukemia (ALL), the number of epigenetic inactivated Eph receptors and ligands was associated with a shortened overall survival.²⁰ In focus of *EphB4* hypermethylation, re-expression of EphB4 by constitutive overexpression in an ALL cell line reduced the leukemic cell proliferation and increased apoptosis. Data on mechanistic consequences related to Eph receptor loss of function is scarce. In this study we aimed to gain detailed biological insight into the Eph receptor signaling in acute myelogenous leukemia (AML).

In this study, we explored the expression of *Eph* receptors and found a common downregulation of *EphB1* assigned to promoter hypermethylation. Interestingly, biolog-

ical insights revealed a tumor suppressor function for EphB1 in AML by coordinating the DNA damage response system. Re-introduction of EphB1 blocked AML cell cycle progression and activated programmed cell death pathways. Clinical consequence of EphB1 suppression in AML was manifested in its association with a longer time to reach a complete remission and a poorer overall survival.

Materials and Methods

Patient samples and AML cell lines. After getting written informed consent the mononuclear cell fraction (MNC) of bone marrow from healthy controls (NBM) and pediatric AML patients was obtained and cryopreserved, approved by the Medical Ethical Committee of the University Medical Center Groningen METC 2010.036 and 2013.281. The cryopreserved bone marrow cells were thawed rapidly at 37°C and diluted in a 6 ml volume of newborn calf serum, as described previously.²¹ The cell lines HL60, THP-1, HEL, NB4 and MOLM13 were obtained from American Type Culture Collection (Manassas, Virginia, USA), cultured in RPMI-1640 medium (Lonza, Basel, Switzerland) supplemented with 1% penicillin/ streptomycin (Life Technologies Europe BV, Bleiswijk, The Netherlands) and 10% fetal calf serum (FCS, Bodinco, Alkmaar, the Netherlands). AML patient samples and AML cell lines all showed severe DNA damage by pH2AX and not in pediatric NBM (Fig. S1A).

Compounds. EfnB1 ligand was used in culture to stimulate EphB1 receptor on AML cells (1 µg/ml recombinant mouse Ephrin B1 ligand, Fc Chimera, R&D systems, Minneapolis, MN, USA). 5-Aza-2'-deoxycytidine (200 nM, Sigma Aldrich, St. Louis, MO, USA) was used as a demethylating agent. Control Fc chimeric protein did not show relevant in vitro effects (data not shown). Etoposide (20mg/ml stock) was used at a concentration of 0.5 µg/ml as a genotoxic agent.

Fluorescence-activated cell sorting (FACS). Cells were blocked by PBS 1% BSA (Bovine Serum Albumin, Sigma Aldrich, St. Louis, MO, USA), and stained with EphB1 antibody (Clone 88512, R&D systems, Minneapolis, MN, USA) or CD34-PE and CD38-PerCP-Cy5.5 antibodies (BD Biosciences, Breda, the Netherlands). Primary EphB1 antibodies were visualized using a Rabbit anti-Mouse PE-conjugated secondary antibody (Dako cytometry, Heverlee, Belgium). For apoptosis analysis, the AML cells were stained with 100 µl of Annexin V/PI solution (1ml staining buffer, with the addition of 20 µl Annexin V-FITC/PE, and 20 µl PI, Roche, Woerden, the Netherlands). For cell cycle analysis cells we fixed in methanol, blocked and incubated with 2 µl phospho-Histone H3 antibody (Cell signaling, Boston, MA, USA) for 20 minutes, washed and stained with 2 µl Propidium Iodide. For proliferation analysis, cells were incubated with BrdU (5-bromo-2'-deoxyuridine) for 4h after which the cells were fixed, denaturated and stained for anti-

Cloning Retroviral vectors. Retroviral supernatants were generated by cotransfection *pMSCV-iGFP* constructs, or *empty vector pMSCV-iGFP*, and packaging plasmid pCLampho into 293T cells by using FuGENE HD transfection reagent (Roche, Woerden, the Netherlands). Transduction efficiency was measured by FACS analysis (Fig. S1C and S2C).

DNA Bisulfite Treatment and Methylation Analysis. DNA was isolated according to manufacturer's (Qiagen, DNA mini kit) protocol. DNA was modified with sodium bisulfite. Bisulfite pyrosequencing and bisulfite sequencing was performed as described previously.²⁰ DNA methylation density ranged from 5-96% for AML cell lines and 1-35% for primary AML (n=21) and NBM (n=5) samples. Primer sequences are included in Table S1.

Gene expression data analysis. The Dutch Childhood Oncology Group (DCOG) pediatric AML cohort gene expression array dataset was used for analyzing EphB1 expression in relation to clinical parameters. Details on gene expression array analysis and the AML patient samples was previously described (GSE22056ID: 200022056).²³ Data for the time to reach a complete remission was available of 79 patient samples. For the overall survival we examined EphB1 (210753_s_at probe with highest coverage of the most unique EphB1 region) gene expression data of 100 pediatric AML samples. The mean EphB1 expression (log2 of 4.59) was used as a cut-off point for the Kaplan-Meier analysis resulting in groups of 42 patients with low EphB1 expression and 58 patients with high EphB1 expression. Validation dataset came from the St. Jude Children's Research Hospital that can be downloaded from the website; <http://www.stjudechildrens.org/site/data/AML1>.²⁴ This dataset contains gene expression data of 97 pediatric AML patient samples divided into t(8;21), INV(16), 11q23, M7 and other cytogenetic subgroups pediatric AMLs with corresponding relapse data. Probe 210753_s_at expression (highest coverage of most unique EphB1 gene region) was log2 transformed to determine differences between favorable and unfavorable cytogenetic subgroups. Favorable cytogenetic subgroups; n=21 for t(8;21) and n=14 for INV(16), and unfavorable; n=23 for 11q23 and n=10 for M7 pediatric AMLs.

Chromatin Immunoprecipitation. 12.5×10^6 treated and untreated THP-1 cells were fixed in 1% formaldehyde for 10 minutes after which glycine (1:20, 2.5M, Sigma Aldrich, St. Louis, MO, USA) was added. A three-step cell lysis was followed by sonification for 10 cycles of 20 seconds. Chromatin immunoprecipitation (Ch-IP) was performed by dis-

solving the nuclei pellets in 110 μ l Chip Buffer (ChIP-IT® Express Chromatin Immunoprecipitation Kit, Active Motif) with protease inhibitors, putting aside 10 μ l input DNA. Lysates were incubated with 2 μ g p53 antibodies (PAb1620 or PAb240 from Abcam, Cambridge, USA) for 4 hours, thereafter, adding 60 μ l Dynabeads® (Life technologies, Bleiswijk, the Netherlands). After reverse cross linking DNA was purified from IP samples and input DNA according to manufacturer's protocol (PCR purification kit, Qiagen).

Cell survival assays. Quantification of leukemia cell viability was carried out using WST-1 assays for AML cell lines. WST-1 assays were performed in triplicates according to manufacturer's protocol (Roche). Cells were seeded at a density of 1×10^5 cells in 100 μ l/well. Mitochondrial activity of AML cell was measured after 48 h using a microplate reader at 450nm (Benchmark; Bio-Rad Laboratories). Cell survival percentages are determined relative to untreated cells.

Statistics. Means and standard deviations of at least three independent evaluations are represented. Statistical package for the social science (SPSS 17) software was used for graphing box-plots. Significant correlations were determined using a Pearson's correlation coefficient (Fig. 1A). The Mann-Whitney U tests were used to determine significant differences between two individual patient groups (as indicated). The Kruskal-Wallis test was used to examine differences between more than two patient groups for significance (as indicated). Unpaired two-tailed Student's t-test was used for all in vitro cell line analysis comparing two conditional experimental groups in at least triplicates. Paired samples T-test was used for determining the overall effect of *EphB1* overexpression in AML cell lines and primary AML samples. Kaplan-Meier analysis was used for defining the cumulative survival based upon high or low EphB1 expression.

Results

EphB1 suppression in AML; a role for DNA methylation

Common genetic deregulation of EphR in cancer pathogenesis urged us to determine the different levels of EphR transcriptional regulation in various AML cell lines. We examined a panel of AML cell lines for their EphA and EphB receptor and EfnB ligand mRNA expression levels in comparison to their promoter methylation density (percentage of CpG sites methylated for the particular gene promoter) using quantitative RT-PCR and bisulfite pyrosequencing respectively (Figure 1A). Interestingly, among EphA and EphB receptors, the promoter of *EphB1* was frequently methylated and presented a unique significant inverse correlation between *EphB1* mRNA expression levels and promoter methylation (Pearson's correlations; $P = 0.717$ for EphA2, $P = 0.841$ for EphA4, $P = 0.301$ for EphA6, $P = 0.256$ for EphA7, $P = 0.010$ for *EphB1*, $P = 0.116$ for *EphB2*, $P = 0.153$ for *EphB3*, $P = 0.198$ for *EphB4*, $P = 0.094$ for *EphB6*, $P = 0.469$ for *EfnB1*, and $P = 0.544$ for *EfnB2*).

EfnB1 mediated growth inhibition and apoptosis of EphB1 expressing AML cells

To gain mechanistic insights into the suppressive role of the EphB1 forward signaling in AML, we investigated the influence of EfnB1 stimulation on AML cell proliferation and survival in AML cell line models. First, we examined EphB1 membrane protein expression in AML cell lines. Approximately 70% of the THP-1 cells express EphB1 on their cell surface (EphB1^{high}), only 25-30% of the HL60 and 10% of the MOLM-13 cells (EphB1^{low}, Figure 1B). EfnB1 stimulation of AML cell lines demonstrated to inhibit the leukemic growth by 50% in EphB1^{high} THP-1 cells as compared to untreated controls (Figure 1C, Student's t-test, $P = 0.001$), but not in EphB1^{low} HL60 and MOLM-13 cells.

Figure 1

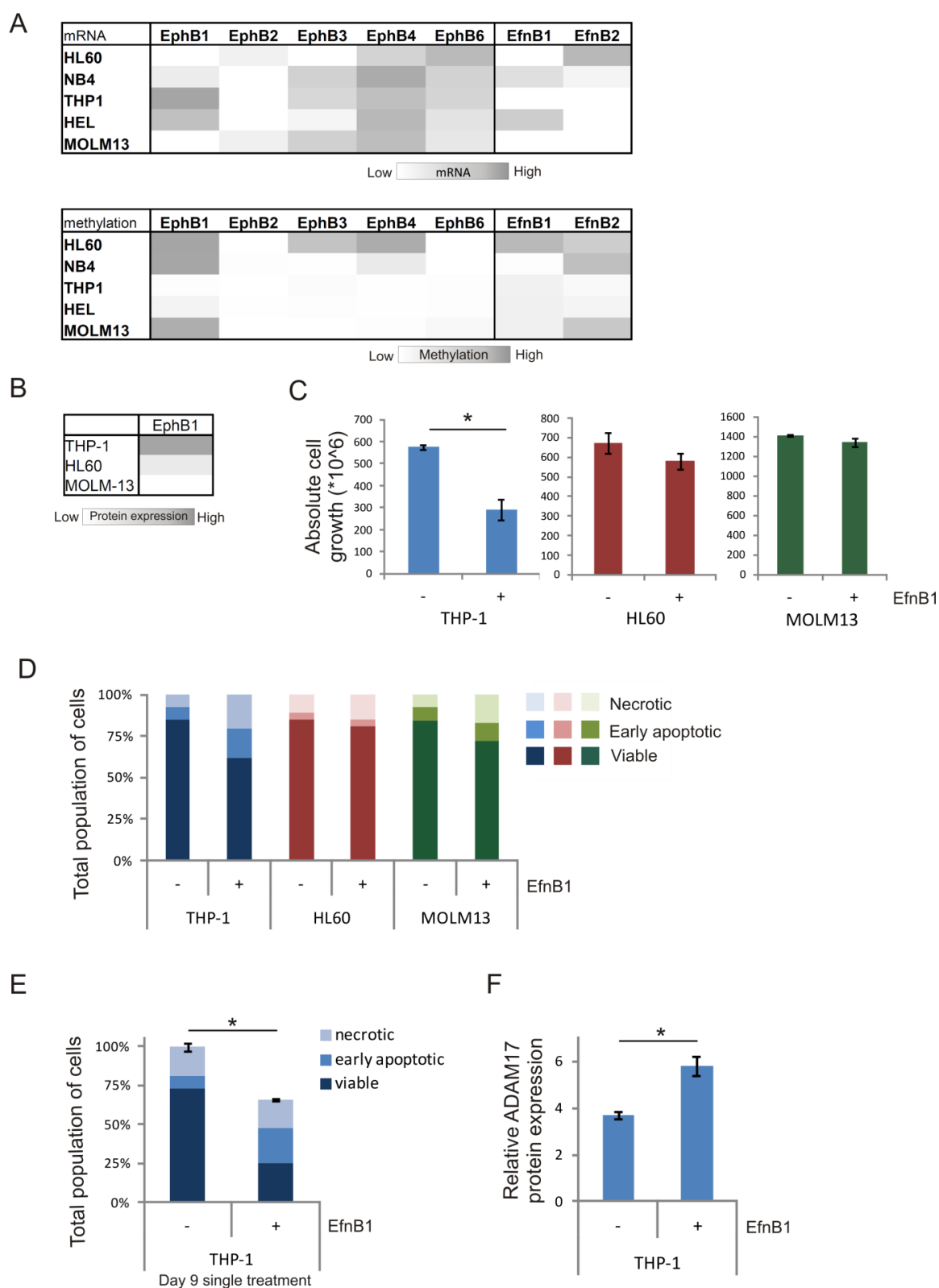


Figure 1. A role for EphB1 suppression in AML; EfnB1 ligand mediated reduction of proliferation and induced apoptosis of AML cells. (A) Heatmap of the mRNA expression levels and methylation density of EphB receptors and EfnB ligands in five AML cell lines, measured using quantitative RT-PCR analysis and

*bisulfite pyrosequencing. (B) A heatmap of flow cytometric EphB1 membrane protein expression levels in AML cell lines (range 10-70% of AML cell line population with EphB1 expression). (C) Growth analysis by absolute cell counts after 72h incubation with EfnB1 in AML cell lines in three independent experiments (mean \pm SEM, * $P = 0.001$). (D) Flow cytometric apoptosis analysis was performed by annexin V/PI staining of 72h EfnB1 stimulated and untreated AML cell lines. (E) Cell survival analysis at day 9 by a single dose of EfnB1 treatment in THP-1 (mean \pm SEM, $P = 0.022$). (F) ADAM17 protein expression measured using ELISA of untreated and EfnB1 treated AML cell lysates after 24h of treatment (mean \pm SEM, $P = 0.015$).*

Next, we examined the effect of EfnB1 stimulation on AML cell survival by Annexin V/PI flow cytometric analysis. EfnB1 stimulation induced programmed cell death by 25% in THP-1 as compared to the untreated controls (Figure 1D). Long-term stimulation with a single dose of EfnB1 reduced the THP-1 AML cell survival by 75% at day 9 (Figure 1E, Student's t-test, $P = 0.029$). To measure EfnB1/EphB1 complex induced cleavage of the receptor in AML cells, we evaluated ADAM17 metalloprotease expression. Determination of ADAM17 revealed that EfnB1 stimulation increased ADAM17 protein expression in THP-1 cells, suggestive for induced EphB1 cleavage (Figure 1F, student's t-test, $P = 0.015$).

EfnB1 induced G2/M cell cycle arrest of EphB1 expressing AML cells

We hypothesized that the phenotypic effects of growth inhibition and the induction of apoptosis could be assigned to a defect in cell cycle regulation. Cell cycle analysis upon EfnB1 ligand stimulation of EphB1^{high} cells revealed an increase in the number of cells in G2/M phase of the cell cycle after which these cells were prone to go into apoptosis (Figure 2A, paired samples t-test, $P = 0.028$). Here, we show that the number of phospho-histone H3 expressing mitotic cells decreased by 40% upon EfnB1 treatment in THP-1 (Figure 2B).

Figure 2

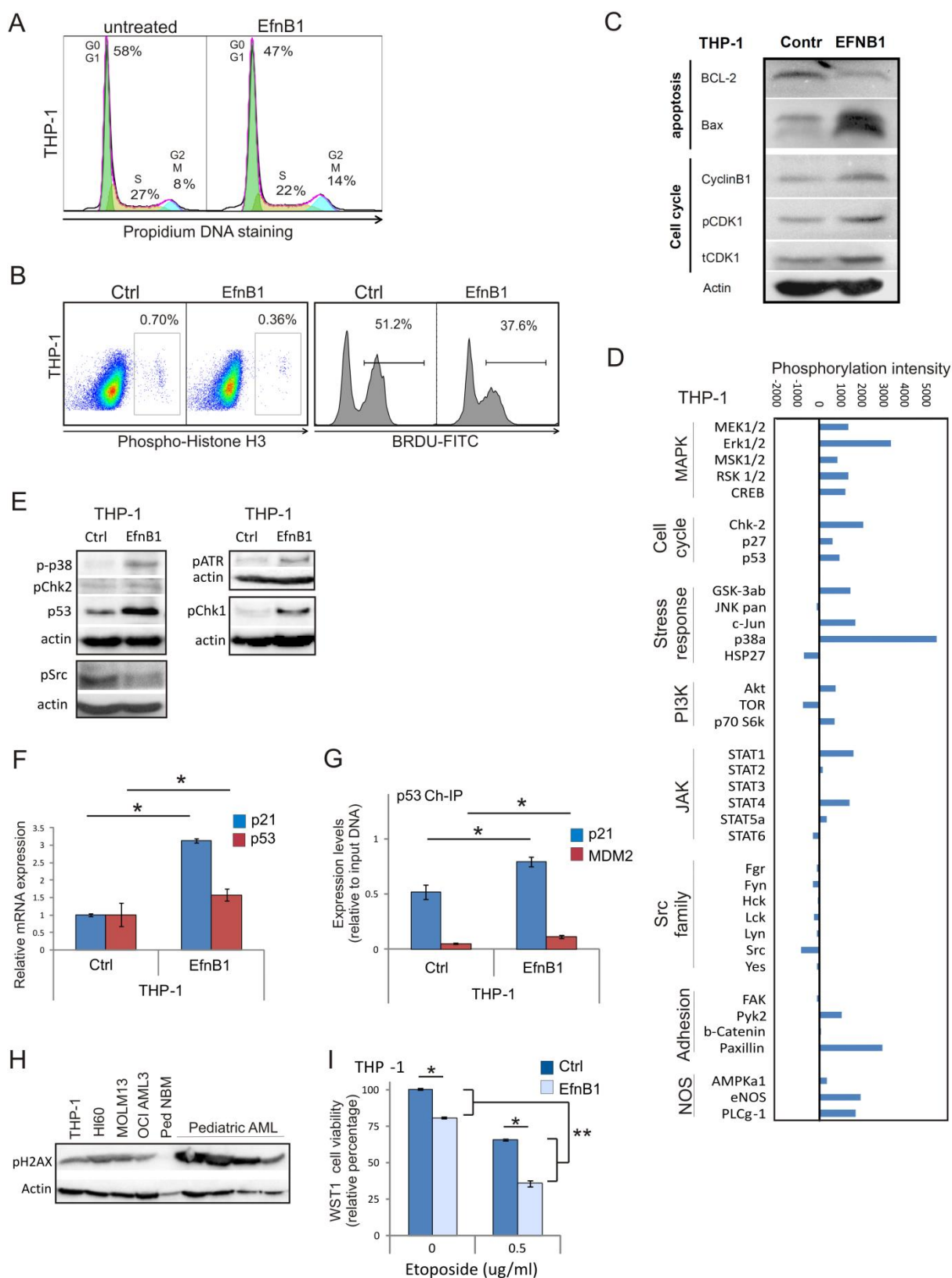


Figure 2. EfnB1 induced G2/M cell cycle arrest is causative for the reduced proliferation and the increased apoptosis in EphB1^{high} THP-1 AML cells.. (A) Flow cytometric analysis of cell cycle compartments by Pro-

*pidium Iodide DNA staining of viable THP-1 cells either untreated or EfnB1 treated for 24h. (B) Flow cytometric analysis of phospho-histone H3 mitotic spindle staining of THP-1 cells either untreated or EfnB1 treated for 24h. (C) Immunoblot analysis of apoptosis and cell cycle regulating proteins; Bcl-2, Bax, CyclinB1, phospho-CDK1^{tyr15}, CDK1, and actin showing the effect of 72h EfnB1 stimulation of THP-1 cells versus untreated control cells. (D) Phosphoproteomic analysis of 72h EfnB1 stimulated THP-1 cells versus untreated control cells. This bar-graph displays the absolute changes in protein kinase phosphorylation upon EfnB1 stimulation of THP-1 cells. (E) Immunoblot analysis of ATR, Chk1, Chk2, p53, p38, and Src phosphorylation in EfnB1 stimulated cells versus untreated THP-1 cells. (F) Quantitative RT-PCR analysis of p21 and p53 in 24h EfnB1 stimulated THP-1 cells versus untreated control cells, confirming the phosphoproteome analysis (mean \pm SEM, * $P < 0.001$). (G) Chromatin immunoprecipitation analysis of p53 in EfnB1 treated THP-1 cells (20h) as compared to untreated controls. Quantitative RT-PCR for p21 and MDM2 was performed to determine p53 DNA binding capacity (mean \pm SEM, * $P < 0.001$). (H) DNA damage defined by phospho- γ H2AX expression by immunoblot analysis of AML cell lines, pediatric normal bone marrow (NBM) control samples, and pediatric AML patient samples. (I) Etoposide induced AML genotoxicity effects on the AML cell survival in untreated and EfnB1 treated THP-1 cells upon 48h treatment, as measured by WST-1 cell survival assay (mean \pm SEM). * significant difference between experimental groups. ** significant additive effects between experimental groups.*

In line with these findings, we observed a 25% reduction in the amount of proliferating cells after 48h EfnB1 treatment and 4h of Brdu incorporation (Figure 2B). Confirming the induction of apoptosis, immunoblot analysis showed a down-regulation of anti-apoptotic Bcl-2 and an induction of pro-apoptotic Bax $_{\alpha/\beta}$ (Figure 2C). Simultaneously, the phosphorylation of the inactivating CDK1 (CDC2) Tyr15-site was up-regulated in EfnB1 stimulated THP-1 cells, which might be initiated by the increased total CDK1 protein levels that we found (Figure 2C). Additionally, CyclinB1 protein expression was enhanced in EfnB1 treated THP-1 cells. Phospho-proteome analysis of untreated and EfnB1 stimulated THP-1 cells unraveled downstream machinery that contributed to the G2/M cell cycle arrest (Figure 2D). As expected, the phosphorylation of cell cycle regulators p27, p38 and p53 was increased upon EfnB1 stimulation of EphB1^{high} AML cells. Moreover, to gain more insights into the observed G2/M cell cycle arrest, we found increased ATR, Chk1, and p38 phosphorylation and p53 total protein expression by EfnB1 stimulation of THP-1 cells, while phosphorylation of Chk2 remained largely unchanged (Figure 2E). Moreover, Src phosphorylation showed to be decreased by EfnB1 treatment in THP-1 cells. In accordance with proteomics, quantitative RT-PCR analysis showed that the expression of *p53* was increased together with downstream cell cycle inhibitor *p21* (Figure 2F, Student's t-test, both *p21* and *p53* $P < 0.001$). Chromatin immunoprecipitation (Ch-IP) of p53 followed by quantitative RT-PCR analysis of p53 distal binding sites on *p21* and *MDM2* revealed that EfnB1 stimulation of THP-1 cells significantly increased the p53 DNA binding capacity (Figure 2G, Student's t-test, both *p21* and *MDM2* $P <$

0.001). EfnB1 induced cell cycle inhibitory effects were not observed in EphB1^{low} HL60 AML cells (Figure S1B).

These data implicate that EfnB1 can induce a G2/M cell cycle arrest in EphB1^{high} AML cells by enhancing p53 DNA binding that prevents the AML cells from entering mitosis and finally results in apoptosis. The restoration of the DNA damage response system upon EfnB1 treatment can only occur in the presence of DNA damage. Therefore, we analyzed phosphorylated γ H2AX levels in the AML. Apparent DNA damage could be observed in AML cell lines and pediatric AML patient samples, but not in the normal bone marrow (NBM) control (Figure 2H). Moreover, EfnB1 stimulation was shown to significantly induce cellular sensitivity to the genotoxic agent etoposide in THP-1 (Figure 2I, Student's t-test, EfnB1 reduced cell survival, * $P < 0.001$).

Programmed cell death as a consequence of EphB1 re-introduction in *EphB1* methylated AML cell lines

Using 5-Aza-2'-deoxycytidine as demethylation treatment in *EphB1* methylated HL60 AML cells we found an increase in EphB1 protein expression by flow cytometry, suggestive for reversible *EphB1* promoter demethylation (Figure 3A, Student's t-test, $P < 0.001$).

To specifically determine whether the EphB1 receptor was indeed the main mediator of the EfnB1 induced cell cycle arrest, we introduced *EphB1* overexpression DNA constructs in the *EphB1* hypermethylated AML cell lines HL60 (*p53*-null) and MOLM13 (*p53*-wildtype), using a constitutive promoter in front of the *EphB1* gene to induce constitutive transcription. An *empty vector* control was used as reference.

Figure 3

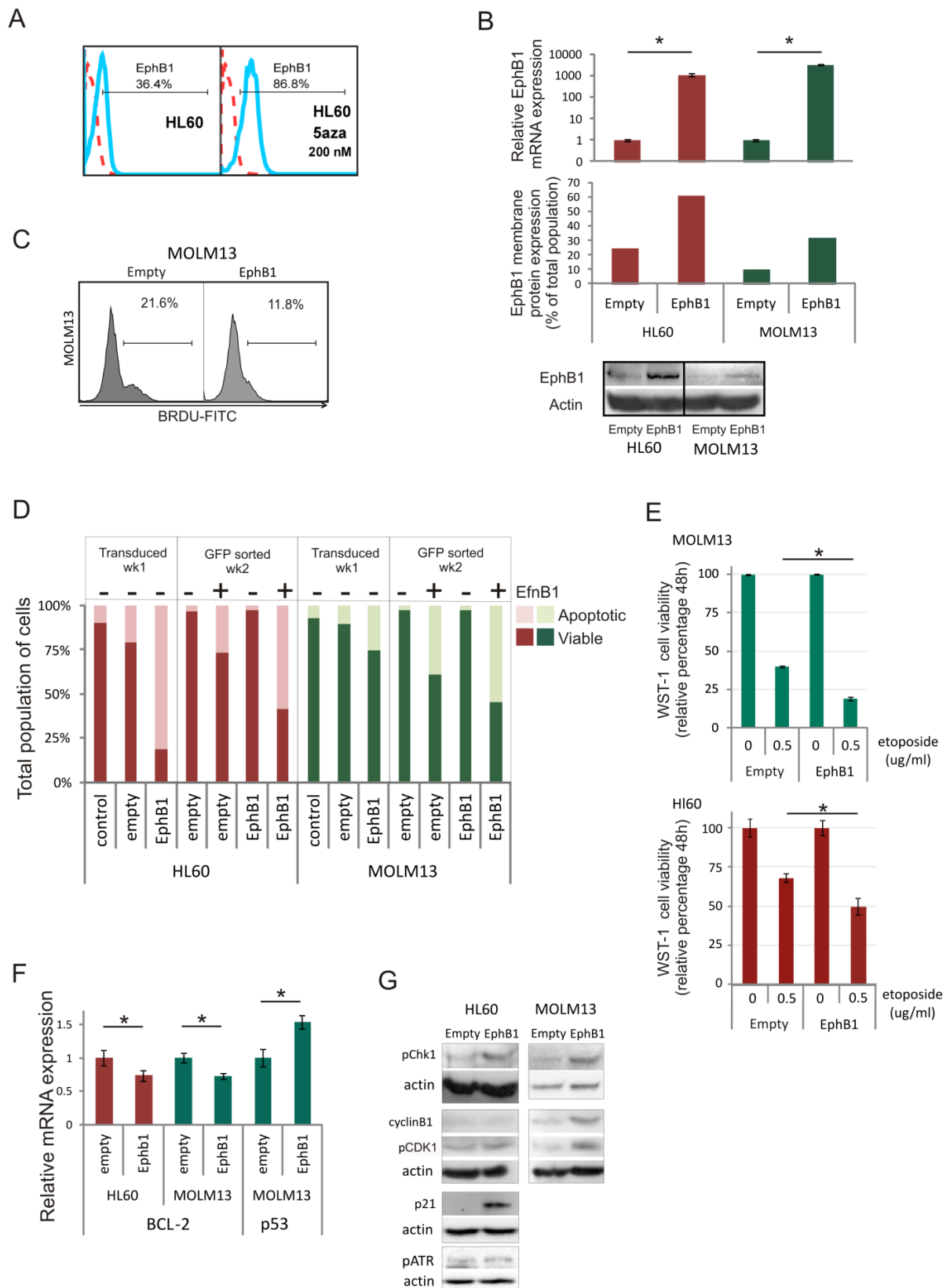


Figure 3. EphB1 overexpression severely induced apoptosis in EphB1 methylated AML cell lines. (A) EphB1

membrane protein expression analysis by flow cytometry after 24h 5-Aza-2'-deoxycytidine treatment of *EphB1* methylated HL60 AML cells. (B) Quantitative RT-PCR analysis of *EphB1* mRNA expression to confirm the *EphB1* overexpression in GFP expressing cells (mean \pm SEM, * $P < 0.001$). Flow cytometric analysis showed that the increased *EphB1* mRNA expression could be translated into induced *EphB1* membrane protein expression in both HL60 and MOLM-13 cells *EphB1* transduced cells. To confirm the induction in *EphB1* protein expression, we simultaneously performed immunoblot analysis of *EphB1*, demonstrating that indeed *EphB1* transduced cells express higher levels of *EphB1* protein. (C) Flow cytometric apoptosis analysis is performed by annexin V-PE staining of 72h EfnB1 treated and untreated transduced HL60 and MOLM13 cells comparing empty vector controls with *EphB1* overexpressing cells. (D) BRDU incorporation analysis for cell proliferation in MOLM13 empty vector controls and *EphB1* overexpression cells (E) Etoposide induced AML genotoxicity effects on the AML cell survival in untreated and EfnB1 treated MOLM13 transduced cells upon 48h treatment, as measured by WST-1 cell survival assay (mean \pm SEM). (F) Quantitative RT-PCR analysis of *Bcl-2* and *p53* comparing EfnB1 treated empty vector control and *EphB1* overexpressing HL60 and MOLM13 cells (mean \pm SEM, * $P < 0.05$). (G) Immunoblot analysis of *pChk1*, *Cyclin B1*, *pCDK1* (Tyr15), *p21*, *pATR* protein expression in empty vector controls and *EphB1* overexpressing HL60 and MOLM13 cells. *significant difference between experimental groups

Re-introduction of constitutive *EphB1* mRNA expression increased *EphB1* transcription by more than 1000-fold in both AML cell lines (Figure 3B, Student's t-test, $P < 0.001$ for HL60 and MOLM13). Flow cytometric analysis showed an induction in *EphB1* membrane expression in both AML cell lines (Figure 3B). Westernblot analysis confirmed the induction of *EphB1* protein expression in *EphB1* overexpression AML cell lines (Figure 3B). Cell cycle progression by Brdu incorporation showed a decreased percentage of proliferating AML cells in *EphB1* overexpression MOLM13 cells (Figure 3C). Re-introduction of *EphB1* into HL60 and MOLM13 cells presented a distinct phenotype, characterized by an increase in apoptosis solely of the *EphB1* transduced populations relatively to *empty vector* control cells (Figure 3D, Figure S1C, Student's t-test, MOLM13 $P < 0.001$). Next, we showed that the remaining viable *EphB1* overexpressing cells were increasingly susceptible to EfnB1 ligand induced apoptosis as compared to *empty vector* controls in both AML cell lines (additional 20-40% increase in apoptosis, Figure 3D). Re-expression and subsequent stimulation of the EfnB1/*EphB1* forward signaling in *EphB1* methylated AML cells markedly decreased the AML cell survival in two independent cell lines (Figure S1D, paired samples t-test, $P = 0.040$, overall apoptosis induction $16\% \pm 12\%$ *empty vector* and $44\% \pm 18\%$ in *EphB1* overexpression cells). Moreover, similar as was observed in THP-1, *EphB1* overexpression MOLM13 and HL60 cells were significantly more sensitive to genotoxicity induced by 48h etoposide treatment (Figure 3E, Student's t-test, $P < 0.001$). Relative mRNA expression of *Bcl-2* was decreased in both *EphB1* overexpressing HL60 and MOLM13 cells (Figure 3F, Student's t-test, $P = 0.014$ and $P = 0.037$). Increased *p53* transcription was evident in *EphB1* overexpressing

MOLM13 cells but not in HL60 *p53*-null cells (Student's t-test, $P = 0.038$). Immunoblot analysis revealed p53-independent regulation of enhanced levels p21 protein expression upon activation of the ATR/Chk1 axis in HL60 *p53*-null cells (Figure 3G). Phosphorylation of downstream CDK1^{tyr15} was enhanced in both HL60 and MOLM13 *EphB1* overexpression cells compared to the *empty vector* control cells (Figure 3G).

EphB1 suppression associated with unfavorable cytogenetics, relapses and decreased probability of overall survival in pediatric AML; a role for *EphB1* methylation

To evaluate whether our proposed model also persists in primary pediatric AML, we extended our analysis from previous study by including normal bone marrow (NBM) controls from the high-throughput kinase activity arrays.²⁵ We showed that kinase activity of the *EphB1* peptide was significantly lower in pediatric AML sample lysates as compared to NBM lysates (Figure 4A/S2A, Mann-Whitney U test, $P = 0.022$). Next, we analyzed *EphB1* mRNA expression levels in a cohort of pediatric AML patient samples ($n=27$) and NBM controls ($n=8$). *EphB1* mRNA expression was found to be significantly reduced in AML as compared to NBM (Mann-Whitney U test, $P = 0.030$). Interestingly, AML samples from patients with cytogenetically unfavorable prognosis showed significantly lowest *EphB1* mRNA expression, followed by samples from patients with other karyotype, while NBM controls presented highest *EphB1* mRNA expression levels (Figure 4B, Kruskal-Wallis test, $P = 0.013$). Validation in a publicly available gene expression dataset of an independent pediatric AML cohort confirmed that *EphB1* expression was significantly lower in cytogenetically unfavorable pediatric AML as compared to favorable AML (Figure S2B, Mann-Whitney U test, $P = 0.008$).

Figure 4

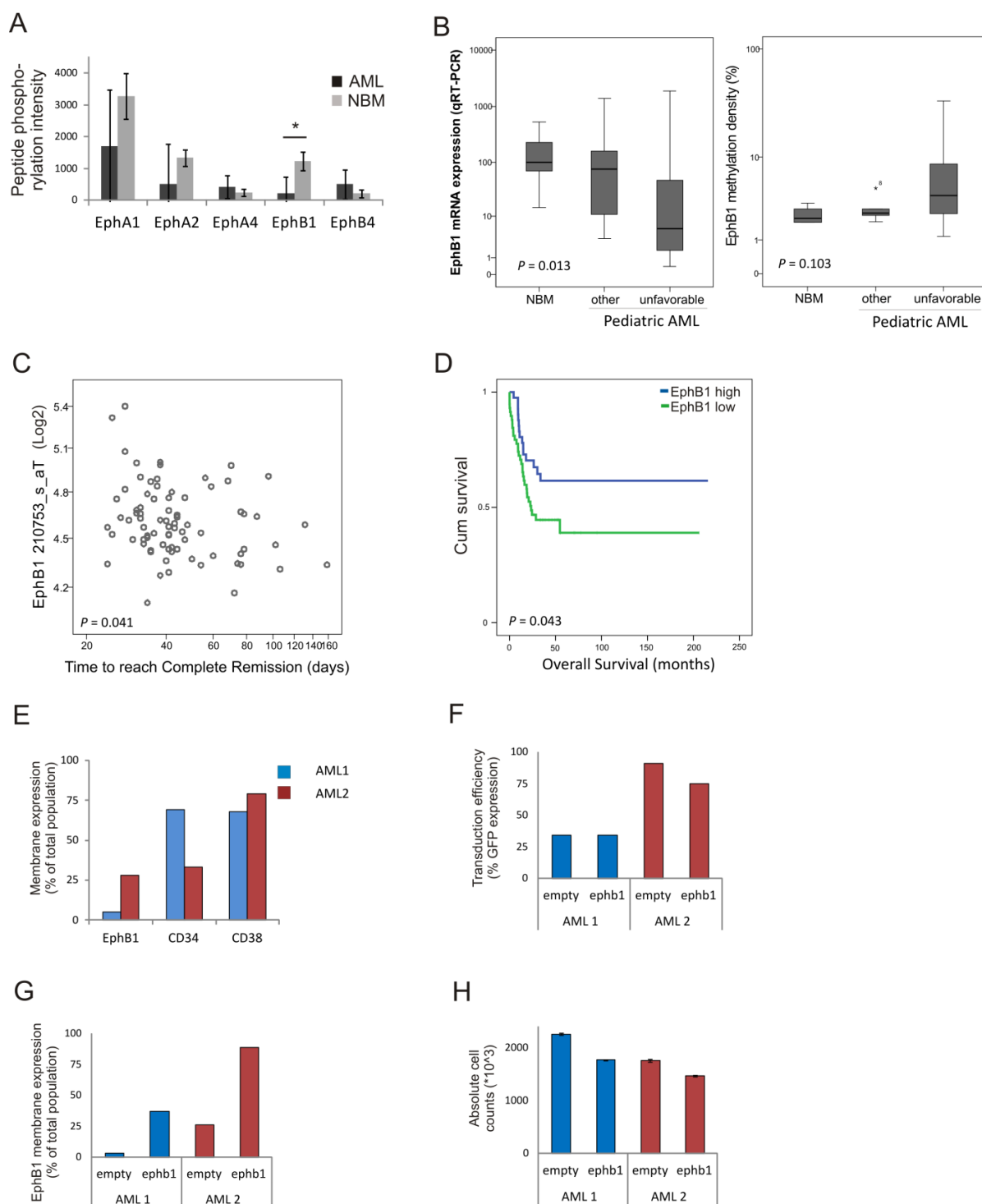


Figure 4. EphB1 suppression in primary pediatric AML. (A) Bar-graph of Ephrin receptor peptide activity in pediatric AML (n=6) and normal bone marrow (NBM) (n=5) lysates (mean \pm SEM, * $P = 0.022$). (B) The left box-plot presenting the mean EphB1 mRNA expression levels as determined using quantitative RT-PCR in NBM controls (n=8), other pediatric AML samples (n=9, NK, INV(16), t(8;21), insertion 8, -9q), and unfavorable AML pediatric patient samples (n=18, complex and 11q23) (mean \pm SEM, $P = 0.013$).

The right box-plot shows the *EphB1* methylation density in NBM controls ($n=4$), other pediatric AML samples ($n=11$) and unfavorable AML pediatric patient samples ($n=10$) (mean \pm SEM, $P = 0.103$). (C) *EphB1* mRNA expression correlated to the time to reach a complete remission using gene expression array analysis of a large pediatric AML cohort ($n=79$, $P = 0.041$). (D) Cumulative survival curve comparing pediatric AML patient samples with high *EphB1* expression versus samples with low *EphB1* expression (with the mean as threshold, high *EphB1* expression $n=42$ and low expression $n=58$, $P = 0.043$). (E) Bar graph of *EphB1*, CD34 and CD38 expression levels in two independent AML patients samples determined by flow cytometry. (F) Flow cytometric analysis of transduction efficiencies after stable introduction of a constitutive *EphB1* overexpression vector in two independent pediatric AML samples. (G) *EphB1* membrane protein overexpression levels in empty vector and *EphB1* overexpression pediatric AML samples using flow cytometric analysis. (H) This bar graph presents the absolute cell counts 7 days after transduction of two primary pediatric AML samples comparing empty vector controls with *EphB1* overexpression vectors (mean \pm SEM).

Bisulfate pyrosequencing revealed increased methylation of the *EphB1* promoter as compared to NBM in 4/21 AML samples. Hypermethylation of the *EphB1* promoter was primarily found in unfavorable AML patient samples (Kruskal-Wallis test, Figure 4B, $P = 0.103$). Using the DCOG pediatric AML gene expression dataset, we found that *EphB1* expression was significantly adversely correlated with the time to reach a complete remission (Figure 4C, Pearson correlation, $P = 0.041$). Interestingly, therapy resistant AML patient samples expressed lower levels of *EphB1* compared to therapy responders (Mann-Whitney U test, $P = 0.026$). Interestingly, the overall survival was associated with *EphB1* expression (Pearson correlation, $P = 0.008$). Pediatric AML patients with low *EphB1* expression showed a significantly reduced overall survival (Figure 4D, Kaplan-Meier, $P = 0.043$).

We challenged to transduce two independent *EphB1*^{low} primary pediatric AML patient samples with our established *EphB1* overexpression construct and the *empty vector* controls. Patient AML1 showed a lack of *EphB1* expression and high CD34 (~70%) and CD38 (~70%) expression levels by flow cytometry (Figure 4E/S2C). Patient AML2 presented low *EphB1* (~27%) and CD34 (~30%) expression levels and high CD38 (~85%) expression levels. Transduction efficiencies were ~35% in AML1 and 75-90% in AML2 (Figure 4F/S2C). *EphB1* overexpression increased membrane protein expression levels by >50% (Figure 4G/S2C). In both AML samples, we found that *EphB1* overexpression reduced the AML cell counts by 20% \pm 3.5% at day 7 after transduction (Figure 4H, paired samples t-test, $P = 0.016$, cell counts $1.45 \times 10^6 \pm 9 \times 10^5$ in empty vector controls and $1.16 \times 10^6 \pm 7 \times 10^5$ in *EphB1* overexpressing AML cells, SEM 3.6×10^5 and 2.9×10^5). These findings may suggest a tumor suppressor function for *EphB1* in primary pediatric AML.

Discussion

Here, we describe that *EphB1* was commonly suppressed in pediatric AML. When EphB1 is present, ligand activation restored the downstream DNA damage response system (p53/p21/Bcl-2) through Chk1 phosphorylation mediated repression of G2 to M transition via CDK1^{tyr15}. *EphB1* re-introduction in EphB1 methylated AML cells operates through similar pathways for cell cycle repression in AML, which allows *p53*-independent routes. The clinical impact of *EphB1* suppression in pediatric AML is illustrated by the enhanced time to reach a complete remission and the association with a reduced overall survival. *EphB1* promoter methylation affected 20% of the pediatric AML samples. These findings emphasize the importance of EphB1 functioning as a tumor suppressor in AML.

A previous study revealed that restoration of ligand induced EphB4 regulated pathways in breast cancer biology is responsible for anti-oncogenic effects in vitro and in vivo.²⁶ Here, we defined the anti-oncogenic effects of *EphB1* re-introduction and ligand stimulatory effects on p53, Chk1, p21, CDK1, Bcl-2 and BAX as important regulatory proteins for downstream EphB1 signaling in AML. The increase in p21 was previously shown to be critical for nuclear retention of the CDK1/CyclinB1 complex by sustained phosphorylation of CDK1^{tyr15}.²⁷ Among the affected pathways are important DNA damage response proteins that facilitate an “anticancer barrier” of normal functioning cells to get rid of or repair DNA damaged cells. The DNA damage response system was found to be commonly defective in AML.²⁸ DNA damage was defined by increased levels of γ -H2AX and phosphorylated ATM in bone marrow biopsies of AML patients that correlated with blast percentages. These proteins were not expressed in healthy bone marrow biopsies. The investigators suggested that AML cells are defective in their DNA damage response system due to inactivation of checkpoint kinases-1/2, which is in accordance with the paradigm established for solid tumors.²⁹ In this study, we found that re-introduction of *EphB1* expression and ligand induced stimulatory signals partly restores the DNA damage control system via Chk1, which forced the AML cells in a G2/M cell cycle arrest. The phenotype of *EphB1* re-introduction was more apparent in AML cell lines compared to primary AML blasts, probably due to the fact that in general cell lines are increasingly DNA damaged during their passages, and their proliferation rate is higher

compared to the primary blasts. The fact that HL60 *p53*-null cells are also vulnerable to *EphB1* reintroduction may imply that EphB1 can also function via *p53*-independent activation of the Chk1/p21 cascade for G2/M suppression.

EphB1 expression is generally low in AML, which could only partially be explained by methylation in 20% of the AML patients. Another contributor may be chromosome 3 alterations in pediatric AML patients. *EphB1* is located on chromosome 3q21. This location is a fragile site region of chromosome 3, and is mainly known to be affected in therapy-related adult AML.³⁰ Chromosome 3 aberrations are rare in pediatrics, but do occur as translocations, inversions and deletions.^{30;31} These genetic alterations may contribute to aberrant expression of *EphB1* in AML patients. Moreover, there are other mechanisms that may interfere with *EphB1* expression. Overexpression of wild-type c-Cbl has been shown to enhance EphB1 ubiquitination and lysosomal degradation.³² This leaves the suggestion that c-Cbl overexpression may contribute to suppression of EphB1 expression and function. However, c-Cbl mutations do not frequently occur in pediatric AML.³³ The tumor suppressor function of EphB1 in AML and the association in a variety of cancers between loss of expression and aggressive tumor phenotypes implies that EphB1 is an important regulator of common cancer cell transforming pathways.^{12;13;34} Conforming, we used the MethHC DNA methylation database in human cancers³⁵ to analyze EphB1 promoter CpG site methylation and found common promoter hypermethylation enriched at the 5'UTR (Fig. S3, all cancers $P < 0.005$). EphB1 promoter hypermethylation was significantly higher as compared to normal sample controls in many cancers including breast, lung, cervical, colon, stomach and prostate cancer. Similar to our NBM samples, the normal tissue sample controls showed no signs of methylation in the EphB1 promoter region.

In this study, we defined the biological and clinical impact of EphB1 as a tumor suppressor in pediatric AML, which encourages further investigation on (epigenetic) mechanisms that regulate EphB1 expression and activation for the development of potential EphB1 inducing therapies.

Acknowledgements

We would like to thank Marcel van Vugt for his expert opinion on DNA damage and cell cycle pathways and the useful discussions. The authors would like to thank the patients who donated leukemia specimens; physician assistants, nurse practitioners, and

fellows who acquired specimens. The authors declare that there is no conflict of interest according to this manuscript.

K.R.K. was supported by a grant from the Foundation for Pediatric Oncology Groningen, the Netherlands (SKOG). S.M.K. was supported by a grant from the Leukemia and Lymphoma society.

Authorship contributions

K.R.K. designed research, performed research, collected data, and wrote the paper. F.J.G. performed research. E.S.J.M.d.B., G.J.K., J.C., C.M.Z., and M.M.v.d.H-E. collaborated within the DCOG consortium to enable the pediatric gene expression array dataset. G.G. and H.Y. performed DNA bisulfite treatment and methylation analysis. S.M.K. supervised paper. E.S.J.M.d.B. designed research, supervised, and wrote the paper.

Reference List

1. Cui XD, Lee MJ, Yu GR et al. EFNA1 ligand and its receptor EphA2: potential biomarkers for hepatocellular carcinoma. *Int.J.Cancer* 2010;126:940-949.
2. Giaginis C, Tsourouflis G, Zizi-Serbetzoglou A et al. Clinical significance of ephrin (eph)-A1, -A2, -a4, -a5 and -a7 receptors in pancreatic ductal adenocarcinoma. *Pathol.Oncol.Res.* 2010;16:267-276.
3. Li X, Wang Y, Wang Y et al. Expression of EphA2 in human astrocytic tumors: correlation with pathologic grade, proliferation and apoptosis. *Tumour.Biol.* 2007;28:165-172.
4. Lu Z, Zhang Y, Li Z et al. Overexpression of the B-type Eph and ephrin genes correlates with progression and pain in human pancreatic cancer. *Oncol.Lett.* 2012;3:1207-1212.
5. Tu Y, He S, Fu J et al. Expression of EphrinB2 and EphB4 in glioma tissues correlated to the progression of glioma and the prognosis of glioblastoma patients. *Clin.Transl.Oncol.* 2012;14:214-220.
6. Foveau B, Boulay G, Pinte S et al. The receptor tyrosine kinase EphA2 is a direct target gene of hypermethylated in cancer 1 (HIC1). *J.Biol.Chem.* 2012;287:5366-5378.
7. Ishikawa M, Miyahara R, Sonobe M et al. Higher expression of EphA2 and ephrin-A1 is related to favorable clinicopathological features in pathological stage I non-small cell lung carcinoma. *Lung Cancer* 2012;76:431-438.
8. Tandon M, Vemula SV, Sharma A et al. EphrinA1-EphA2 interaction-mediated apoptosis and FMS-like tyrosine kinase 3 receptor ligand-induced immunotherapy inhibit tumor growth in a breast cancer mouse model. *J.Gene Med.* 2012;14:77-89.
9. Yang NY, Fernandez C, Richter M et al. Crosstalk of the EphA2 receptor with a serine/threonine phosphatase suppresses the Akt-mTORC1 pathway in cancer cells. *Cell Signal.* 2011;23:201-212.
10. Noblitt LW, Bangari DS, Shukla S et al. Decreased tumorigenic potential of EphA2-overexpressing breast cancer cells following treatment with adenoviral vectors that express EphrinA1. *Cancer Gene Ther.* 2004;11:757-766.
11. Noblitt LW, Bangari DS, Shukla S, Mohammed S, Mittal SK. Immunocompetent mouse model of breast cancer for preclinical testing of EphA2-targeted therapy. *Cancer Gene Ther.* 2005;12:46-53.
12. Wang H, Wen J, Wang H et al. Loss of expression of EphB1 protein in serous carcinoma of ovary associated with metastasis and poor survival. *Int.J.Clin.Exp.Pathol.* 2014;7:313-321.
13. Wang JD, Dong YC, Sheng Z et al. Loss of expression of EphB1 protein in gastric carcinoma associated with invasion and metastasis. *Oncology* 2007;73:238-245.
14. Guan M, Xu C, Zhang F, Ye C. Aberrant methylation of EphA7 in human prostate cancer and its relation to clinicopathologic features. *Int.J.Cancer* 2009;124:88-94.
15. Oba SM, Wang YJ, Song JP et al. Genomic structure and loss of heterozygosity of EPHB2 in colorectal cancer. *Cancer Lett.* 2001;164:97-104.
16. Pasquale EB. Eph receptors and ephrins in cancer: bidirectional signalling and beyond. *Nat.Rev.Cancer* 2010;10:165-180.
17. Alazzouzi H, Davalos V, Kokko A et al. Mechanisms of inactivation of the receptor tyrosine kinase EPHB2 in colorectal tumors. *Cancer Res.* 2005;65:10170-10173.
18. Fox BP, Kandpal RP. Transcriptional silencing of EphB6 receptor tyrosine kinase in invasive breast carcinoma cells and detection of methylated promoter by methylation specific PCR. *Biochem.Biophys.Res.Comm.* 2006;340:268-276.
19. Jin W, Qi S, Luo H. The effect of conditional EFNB1 deletion in the T cell compartment on T cell development and function. *BMC.Immunol.* 2011;12:68.
20. Kuang SQ, Bai H, Fang ZH et al. Aberrant DNA methylation and epigenetic inactivation of Eph receptor tyrosine kinases and ephrin ligands in acute lymphoblastic leukemia. *Blood* 2010;115:2412-2419.

21. Dokter WH, Tuyt L, Sierdsema SJ, Esselink MT, Vellenga E. The spontaneous expression of interleukin-1 beta and interleukin-6 is associated with spontaneous expression of AP-1 and NF-kappa B transcription factor in acute myeloblastic leukemia cells. *Leukemia* 1995;9:425-432.
22. Kampen KR, Ter Elst A, Mahmud H et al. Insights in dynamic kinome reprogramming as a consequence of MEK inhibition in MLL-rearranged AML. *Leukemia* 2014;28:589-599.
23. de Jonge HJ, Valk PJ, Veeger NJ et al. High VEGFC expression is associated with unique gene expression profiles and predicts adverse prognosis in pediatric and adult acute myeloid leukemia. *Blood* 2010;116:1747-1754.
24. Ross ME, Mahfouz R, Onciu M et al. Gene expression profiling of pediatric acute myelogenous leukemia. *Blood* 2004;104:3679-3687.
25. Ter Elst A, Diks SH, Kampen KR et al. Identification of new possible targets for leukemia treatment by kinase activity profiling. *Leuk.Lymphoma* 2011;52:122-130.
26. Noren NK, Foos G, Hauser CA, Pasquale EB. The EphB4 receptor suppresses breast cancer cell tumorigenicity through an Abl-Crk pathway. *Nat.Cell Biol.* 2006;8:815-825.
27. Satyanarayana A, Hilton MB, Kaldis P. p21 Inhibits Cdk1 in the absence of Cdk2 to maintain the G1/S phase DNA damage checkpoint. *Mol.Biol.Cell* 2008;19:65-77.
28. Boehrer S, Ades L, Tajeddine N et al. Suppression of the DNA damage response in acute myeloid leukemia versus myelodysplastic syndrome. *Oncogene* 2009;28:2205-2218.
29. Lord CJ, Ashworth A. The DNA damage response and cancer therapy. *Nature* 2012;481:287-294.
30. Lindquist R, Forsblom AM, Ost A, Gahrton G. Mutagen exposures and chromosome 3 aberrations in acute myelocytic leukemia. *Leukemia* 2000;14:112-118.
31. Tchinda J, Dijkhuizen T, Vlies PP, Kok K, Horst J. Translocations involving 6p22 in acute myeloid leukaemia at relapse: breakpoint characterization using microarray-based comparative genomic hybridization. *Br.J.Haematol.* 2004;126:495-500.
32. Fasen K, Cerretti DP, Huynh-Do U. Ligand binding induces Cbl-dependent EphB1 receptor degradation through the lysosomal pathway. *Traffic.* 2008;9:251-266.
33. Coenen EA, Driessen EM, Zwaan CM et al. CBL mutations do not frequently occur in paediatric acute myeloid leukaemia. *Br.J.Haematol.* 2012;159:577-584.
34. Teng L, Nakada M, Furuyama N et al. Ligand-dependent EphB1 signaling suppresses glioma invasion and correlates with patient survival. *Neuro.Oncol.* 2013;15:1710-1720.
35. Huang WY, Hsu SD, Huang HY et al. MethHC: a database of DNA methylation and gene expression in human cancer. *Nucleic Acids Res.* 2015;43:D856-D861.

Supplementary data

Supplementary Figure 1

A

mRNA	EphA2	EphA4	EphA6	EphA7	EphB1	EphB2	EphB3	EphB4	EphB6	EfnB1	EfnB2
HL60	0	0	0,142473	3,146375	0	2,052349	0	6,153936	9,502341	0	9,740219
NB4	0	0	0	5,356868	2,651645	0	6,408002	11,605	6,2597	4,445735	1,524186
THP1	0	0	0,584668	7,898197	12,34096	0	5,621923	8,819536	6,01497	0	0
HEL	0	0	0	0	8,721059	0	1,443571	9,75562	3,864655	6,88564	0
MOLM13	0	0	0	0	0	2,133115	6,554043	9,172855	3,331945	0	0
methylation											
HL60	74,41	90,01	81,69	85,28	94,79	1,91	64,33	88,3	1,33	74,89	53,47
NB4	68	90,48	84,75	29	93,77	3,45	2,54	23,52	1,67	4,32	67,9
THP1	5,94	52,62	4,3	1,2	3,97	2,2	5,67	2,71	4	16,23	8,25
HEL	24,18	5,8	13,36	72,99	14,52	3,36	3,47	3,38	4,4	17,45	13,21
MOLM13	12,56	63,21	72,85	33,88	85,74	1,8	1,61	3,8	8,69	16,98	58,49

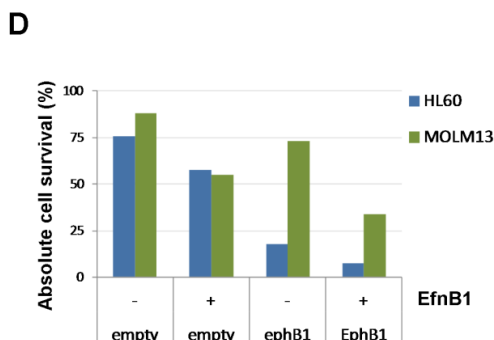
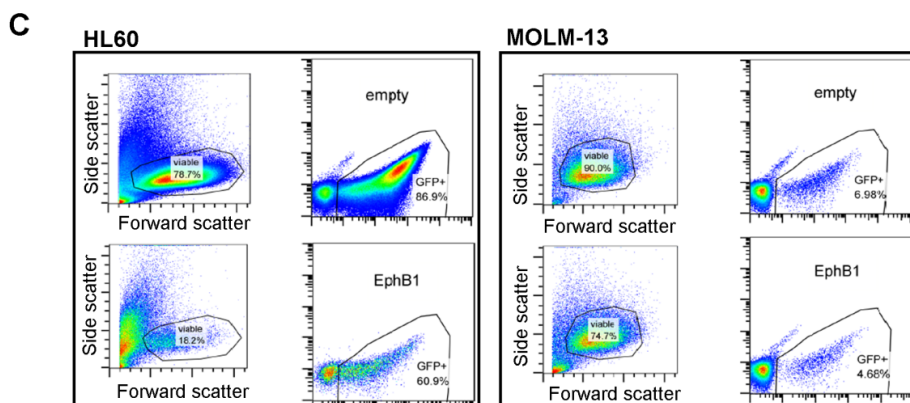
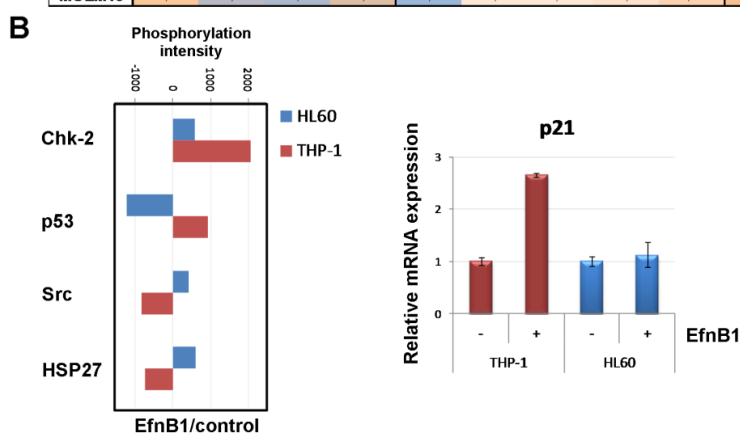


Figure S1. EfnB1 stimulated AML cells under different conditions. (A) Relative EphA and EphB receptor and EfnB ligand mRNA expression in AML cell lines and subsequent methylation density analysis (% gene promoter methylation). (B) Effects of EfnB1 stimulation of THP-1 and HL60 cells on the phosphorylation of Chk-2, Src, p53, and HSP27 as compared to untreated control cells. Quantitative RT-PCR analysis of p21 in THP-1 and HL60 upon EfnB1 stimulation. (C) GFP cell sorting of HL60 and MOLM-13 transduced cells showed an extreme induction in apoptosis of EphB1 transduced HL60 and MOLM-13 cell populations as compared to empty vector controls (comparing the viable populations). The drop in GFP percentage of the viable population provides an additional indication that EphB1 introduction into AML cells induced AML cell death instantly. Viable cells in the GFP gates were sorted for further analysis. (D) The absolute cell survival effect of EphB1 introduction and subsequent EfnB1 treatment effects on GFP sorted AML HL60 and MOLM-13 cell survival between empty vector and EphB1 overexpressing cells.

Supplementary Figure 2

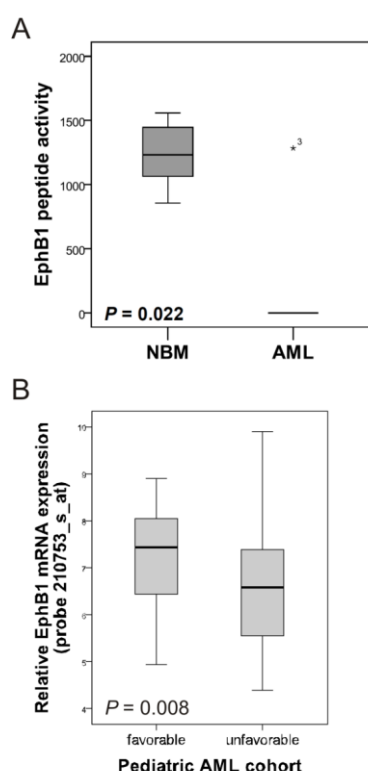
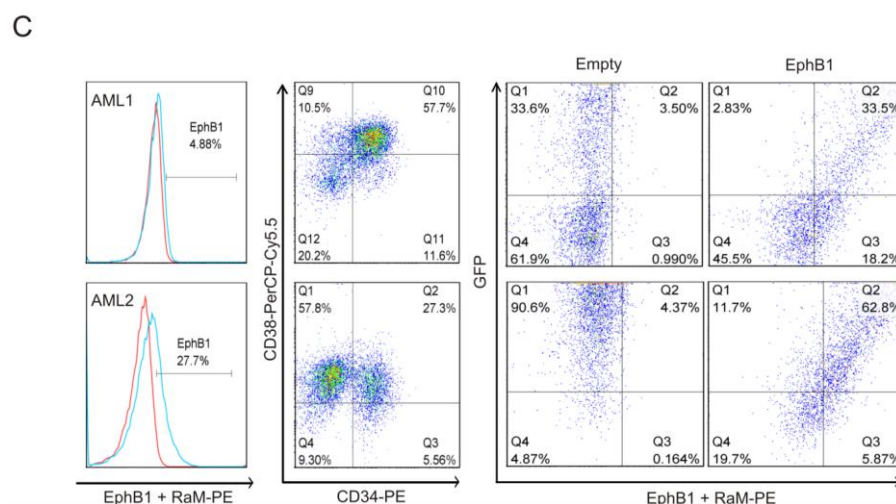


Figure S2. EphB1 suppression in pediatric AML. (A) Box-plot of EphB1 peptide activity in pediatric AML (n=6) and NBM (n=5) lysates. (B) EphB1 expression from gene array data of St. Jude Children's Hospital (n=129) for probe 210753_s_at comparing the favorable versus the unfavorable pediatric AML patient groups. (C) Flow cytometric analysis for EphB1, CD34 and CD38 membrane protein expression in pediatric AML samples used for re-introduction of EphB1, which is shown at the right side dot-plots.



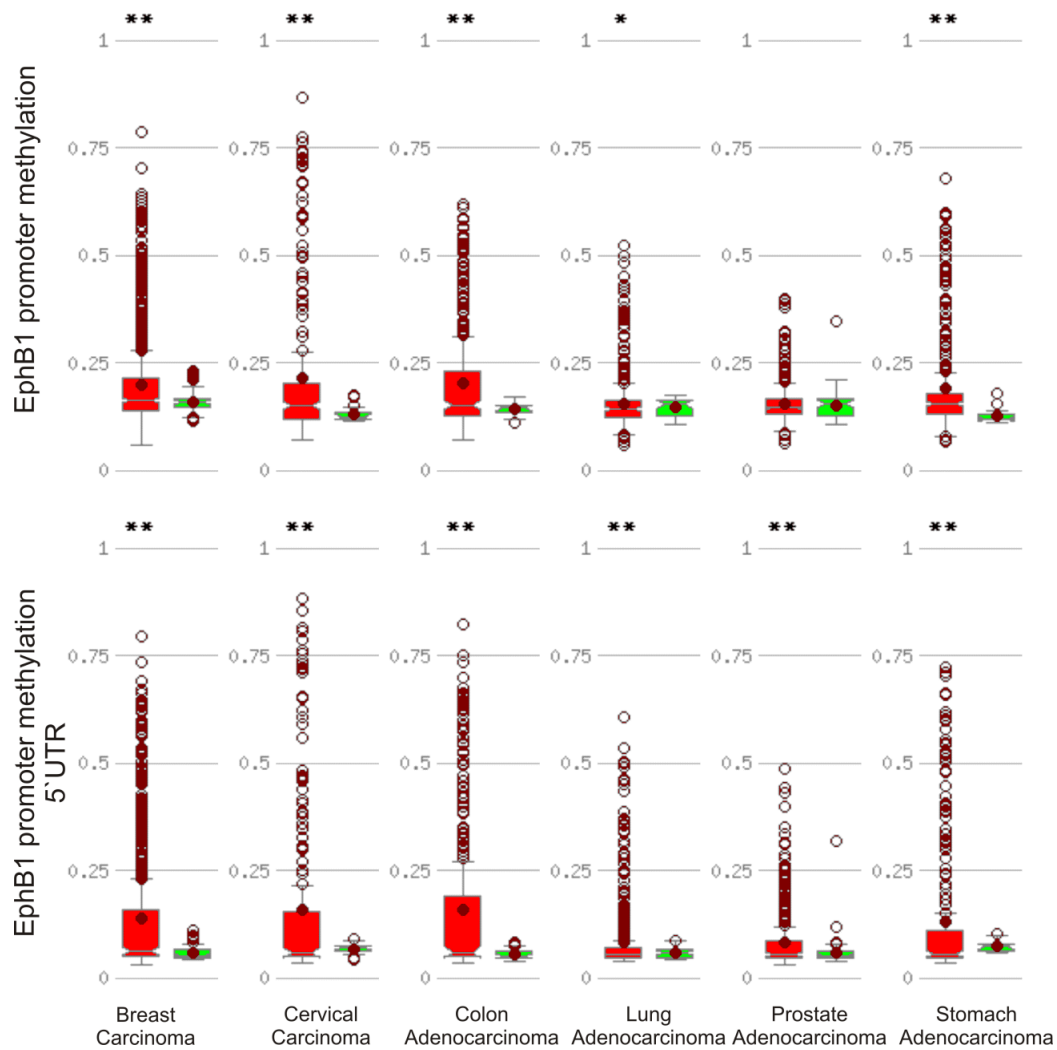


Figure S3. EphB1 promoter methylation in cancer. EphB1 methylation analysis from MethHC database presenting DNA methylation of the EphB1 promoter (*, $P < 0.050$, ** $P < 0.005$). The red boxes represent tumor samples and green boxes depict the normal tissue samples. A ratio value of 0 equals to non-methylation of the locus, a ratio of 1 equals to total methylation, and a value of 0.5 means that one copy is methylated and the other is not, in the diploid human genome.

Table S1. Primer sequences.

		Forward	Reverse
mRNA	HPRT	TTGCTGACCTGCTGGATTAC	CCCTGTTGACTGGTCATTAC
	EphB1	CTT TGA CCC TCC AGA AGT GG	CTCCACATTGTCGTCACAGC
	p21	GGC AGA CCA GCA TGA CAG ATT	AGAGGAAGCCCTAATCCG
	p53	GAGATGTTCCGAGAGCTGAATGAGGC	TCTTGAACATGAGTTTTTTA
	Bcl-2	GAGGCTGGGATGCCTTTGTG	TGGCGGGAGG
DNA			GGGCCAAACTGAGCAGAGTC
	p21	AACATGCTTGGGCAGCAGGC	AGCCACCAGCCTCTTCTATGCCA
	MDM2	TTGAGCTGGTCAAGTTCAGACACG	AGCCCCAGCTGGAGACAAGTCAG
	GAPDH	GGTGGTCTCCTCTGACTTCAACA	GTGGTCGTTGAGGGCAATG

Bisulfite	EphB1	AGAGAGTGAGTTTGGTGTTA	CCCCAAAAATTTTACAAA
PCR		TATTGTTAGT	TTTAATTCCTT

